



Nondestructive measurement of nanofiber diameters using microfiber tip

PENGFEI ZHANG,^{1,2,*} FAN CHENG,¹ XIN WANG,¹ LIJUN SONG,¹ CHANG-LING ZOU,^{3,1} GANG LI,^{1,2} AND TIANCAI ZHANG^{1,2}

¹State Key Laboratory of Quantum Optics and Quantum Optics Devices, Institute of Opto-Electronics, Shanxi University, Taiyuan 030006, China

²Collaborative Innovation Center of Extreme Optics, Shanxi University, Taiyuan, Shanxi 030006, China

³Key Laboratory of Quantum Information, CAS, University of Science and Technology of China, Hefei, Anhui 230026, China

*zhangpengfei@sxu.edu.cn

Abstract: We demonstrate a convenient and simple method to determine nanofiber diameters nondestructively using a hemispherical microfiber tip probe. For a fixed-tip geometry and working wavelength, the scattering losses of nanofiber transmission induced by the tip are a function of the nanofiber diameter, while being insensitive to the alignment. Therefore, the nanofiber diameter can be estimated based on the measured nanofiber transmittance and the loss-diameter relationship that are obtained by three-dimensional numerical simulations. The method is experimentally demonstrated with a diameter measurement precision of 9.8 nm (1.5% of the measured diameter), and the results agree with those obtained by other methods. Such a nondestructive near-field probe approach offers a reliable and convenient technique for determining nanofiber diameters, with applications ranging from optical sensing to quantum optics to quantum information processing.

© 2018 Optical Society of America under the terms of the [OSA Open Access Publishing Agreement](#)

1. Introduction

During the past decade, microfibers and nanofibers have been a topic of great interest and a versatile photonic platform with enhanced light-matter interactions and high photon collection efficiency [1–4]. Therefore, nanofibers have been widely applied in applications ranging from photonic devices [5,6] to optical sensing [1] to quantum optics [7] to quantum information processing [8]. In many of the applications mentioned above, the nondestructive determination of nanofiber diameters is essential and significant. For the enhanced photon-emitter coupling in nanofibers, an optimal diameter is on-demand for maximizing the electric field at the surface of the nanofiber [9,10]. When fabricating the in-line nanofiber photonic microstructures, the nanofiber diameters have a critical effect on the resonance frequency of photonic crystal cavities on optical nanofibers [11–13]. In applications in which there are trapping atoms around the nanofiber, a waist region with a uniform and optimized diameter is often required [14–16]. Scanning electron microscopy (SEM) with nanometer resolution is a powerful tool to profile nanofibers and to determine the diameter; however, it is destructive because the conductive coating required by SEM measurements will damage the surface of nanofibers. In addition, SEM is time-consuming and requires specific facilities, and the sample-transferring process for SEM may break the nanofiber.

To avoid destructive SEM measurements, several techniques to measure nanofiber diameters based on complex diffraction pattern [17], composite photonic crystal cavity [18], second- and third-harmonic generation [19], modal interference [20], tensile force-elongation [21], Brillouin scattering [22] and Rayleigh scattering [23] are proposed and demonstrated. In 2006, Sumetsky *et al.* devised a simple technique for probing the optical microfiber surface and bulk distortions with sub-nanometer accuracy [24]. In this method, a partly stripped regular optical fiber was used as a probe that slides along a microfiber transmitting the

fundamental mode, and the nanofiber transmission with scattering loss is detected. Thus, the variation of the effective microfiber radius can be determined based on the transmission of nanofibers. Although this method cannot determine the absolute diameters of nanofibers, Madsen *et al.* demonstrated a method for absolute diameter determinations using another nanofiber for a probe [25] based on an idea suggested by Sumetsky *et al.* [24]. However, the absolute size calibration based on multimode interference behavior in the tapered section is demanding for sub-nanometer radial resolution. Therefore, it is challenging in experiments to determine the nanofiber diameter nondestructively and reliably.

In this paper, we propose and demonstrate a novel method to estimate nanofiber diameters based on near-field probe-induced scattering. The key idea is that the near-field scattering loss depends on the evanescent field of the nanofiber, which is determined by the diameter of the nanofiber. In our experiments, a microfiber tip (MFT) measuring tens of micrometers is selected as the near-field probe with which to touch the nanofibers and induce nanofiber scattering loss. MFTs with large diameters can be fabricated easily and the diameters can be measured precisely using an optical microscope, and its spherical tip shape indicates that the scattering loss is insensitive to alignment imperfection. Therefore, the scattering loss in such a nanofiber-MFT system can be precisely simulated by the three-dimensional (3D) finite-difference time-domain (FDTD) method, and the relationship between the nanofiber transmissions and the diameters can be obtained. As a result, the nanofiber diameters can be estimated based on the measured transmittance and simulated relationship. Our method does not need extra experimental measurement to calibrate the experimental results. The nanofiber diameter can be estimated directly according to the experimental results of nanofiber transmission and FDTD simulation quickly. It is worth noting that the simulation results presented in this paper can be used for our future measurement and can be shared with whom want to use this technique, so no further FDTD simulations are needed for future calibration. In addition, it is convenient to determine the nanofiber diameter quickly when we want to determine the nanofiber diameter at one point or few points along a nanofiber. The numerical simulation calibration makes this technique convenient and simple and the point touching makes it nondestructive; thus, our approach demonstrated here is useful for practical experiments.

2. Principle and theoretical simulations

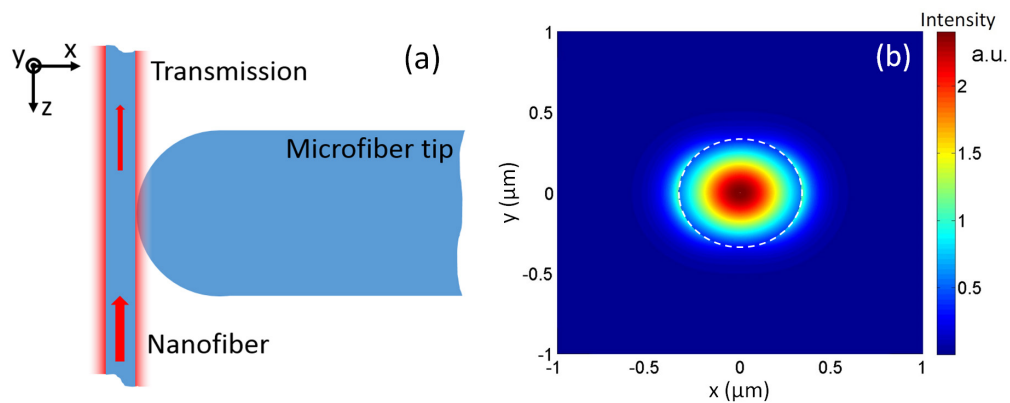


Fig. 1. (a) Schematic of a nanofiber with a MFT touching. The figure is not drawn to scale. (b) Total intensity distribution $|E|^2$ of the electric field in x-y plane (cross-section of the nanofiber) for the fundamental HE_{11} mode, i.e., the TM mode. Nanofiber diameter is 670 nm, while the vacuum wavelength of guided mode is 852 nm.

Figure 1(a) is a schematic of the proposed nondestructive approach for measuring the diameter of a nanofiber, in which a hemispherical MFT is perpendicularly touching the

nanofiber. Since the diameter of the nanofiber is comparable with the wavelength, there is a considerable portion of the energy of the optical guide mode outside the dielectric in the form of an evanescent wave. Figure 1(b) shows the numerically solved electric-field intensity distribution of the fundamental HE_{11} transverse-electric (TM mode) mode of a nanofiber, with a nanofiber diameter of 670 nm and a guided-mode vacuum wavelength of 852 nm. TM mode is of the quasi-linear polarization along the x-axis of fundamental HE_{11} mode family, while TE mode is along the y-axis. From Fig. 1(b), it can be seen that a strong evanescent field extends out into the surrounding air. Therefore, when a hemispherical MFT touches the nanofiber, the evanescent wave will be scattered by the near-field probe, and the transmittance of the nanofiber will drop. Here, we propose to monitor the transmission of the nanofiber and determine its diameter for a fixed probe size and input light wavelength.

The 3D FDTD method (Lumerical Solutions, Inc.) is applied to numerically simulate the nanofiber transmission with a hemispherical MFT touching as shown in Fig. 1(a). Figure 2(a) shows the normalized transmission of the nanofiber as a function of nanofiber diameter d_{fiber} , with different MFT diameters d_{tip} from 2 to 52 μm and a fixed wavelength of 852 nm of the TM-polarized input light. Due to the scattering, nanofiber transmission is reduced. The results indicate that: (i) the scattering loss present for the nanofiber diameter is comparable with the wavelength, and evanescent wave outside the nanofiber surface can be scattered greatly by the MFT. (ii) loss monotonically increases with MFT size for all of the nanofiber diameters, and (iii) the curves for different MFT sizes converge when d_{tip} exceeds 40 μm . To clearly illustrate the convergence, in Fig. 2(b) we plot the loss dependence on d_{tip} for fixed nanofiber size as well as the maximum scattering. These behaviors can be understood as the scattering loss increases the overlap between the evanescent field and the MFT, and thus smaller nanofiber diameters enhance the evanescent field and, in turn, the loss. A larger MFT size also leads to larger loss and saturates as a large-diameter MFT can be treated as a flat substrate. However, the scattering loss is suppressed if d_{fiber} is small enough. This might be attributed to the fact that the optical field is delocalized around the nanofiber when d_{fiber} is small enough. When the diameter of the nanofiber is very small (such as smaller than 100nm), the light can be only weakly confined in the dielectric and most of the light is in the air. We can intuitively understand the constant (~40%) transmission of nanofiber when touch with the MFT as: the weakly confined light can be treated as a free-space beam that shining on the MFT. Since only half of the beam cross-section is blocked by the MFT, we can still have a considerable portion of light pass the MFT due to the diffraction effect. Sudden changes of nanofiber transmission shown in Fig. 2 (a) for 52 μm and 40 μm happen at around nanofiber diameter of 850nm, while the wavelength of guided light is 852nm. The features are mainly attributed to two reasons. One is the effect of the multimode guided in thick nanofibers. Another one is that an unexpected resonance happens. We did not observe sudden changes of nanofiber transmission for nanofiber diameter 850nm in the experiments. Therefore, we guess the sudden changes of nanofiber transmission will only happen at some rigorous condition in theory.

From Fig. 1(b), we note that the transverse intensity distribution is not cylindrically symmetric. The intensity distribution is twofold-symmetrical and the quasilinear polarization strongly depends on the azimuthal angle. We plot the nanofiber transmission as a function of nanofiber diameters for TE and TM modes (modes with y and x polarization), shown in Fig. 2(c). It can be seen that polarizations of the guided mode have a very small effect on the nanofiber transmission for $d_{tip} = 52 \mu\text{m}$. We keep the TM mode (x polarization) in the following simulations optionally. The nanofiber transmissions drop to lowest values (minimum is almost zero) for very small d_{fiber} and the nanofiber transmission increases when

d_{fiber} is further reduced. Figure 2(d) shows the normalized nanofiber transmission as a function of nanofiber diameter with different wavelengths of guided modes when d_{tip} is 52 μm .

All of these numerical results show that nanofiber transmission increases monotonically when d_{fiber} is bigger than the diameter corresponds to the minimum of the nanofiber transmission shown in Fig. 2; therefore, the nanofiber diameter can be estimated from the experimental transmission data. Choosing the wavelength of laser sources would allow great flexibility in measurement range. Broadband light sources would present a measurement with a large range of nanofiber diameters. Furthermore, we can fabricate MFTs with large diameters easily and measure the diameters precisely using an optical microscope, which is beneficial for experimental manipulation.

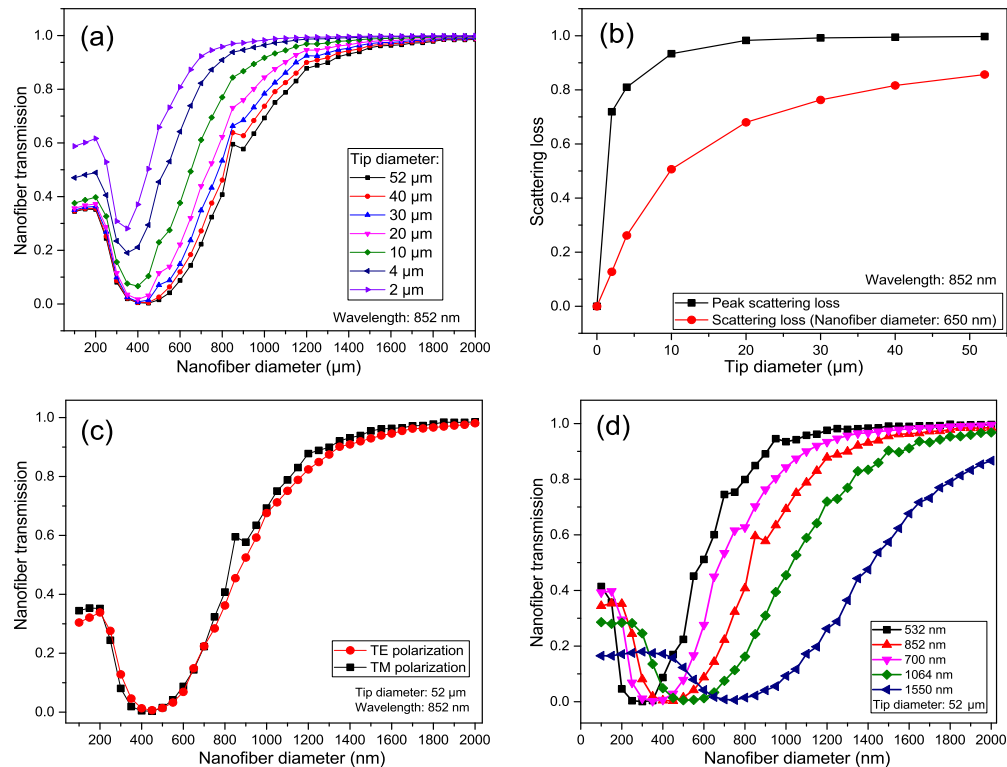


Fig. 2. (a) Nanofiber transmission as a function of nanofiber diameter with different MFT diameters from 2 to 52 μm . Vacuum wavelength of the guided mode is 852 nm. See [Data File 1](#) for underlying values. (b) Scattering loss with nanofiber diameter 650 nm and the maximum scattering loss as a function of MFT diameter. (c) Nanofiber transmission as a function of nanofiber diameter for TE and TM modes (modes with y and x polarization). MFT diameter is 52 μm . (d) Nanofiber transmission as a function of nanofiber diameter with different wavelengths of guided modes (532, 852, 700, 1064, and 1550 nm). MFT diameter is 52 μm for (c) and (d).

3. Experimental results

The experimental setup for nondestructive measurement of nanofiber diameters using a hemispherical MFT is shown schematically in Fig. 3(a). A laser beam is collimated and coupled into an optical single mode fiber by a fiber coupler. The light passes through a tapered optical fiber and the power of output light is measured by a detector. The tapered optical fiber is fabricated from a single-mode fiber (SM800, Fibercore) by the flame-brush

method [26]. Our flame-brush setup consists of two computer-controlled, high-precision motors to pull and narrow the single-mode optical fiber melted by a traveling hydrogen/oxygen flame. Figure 3(c) shows a typical scanning electron microscope (SEM) image of the nanofiber.

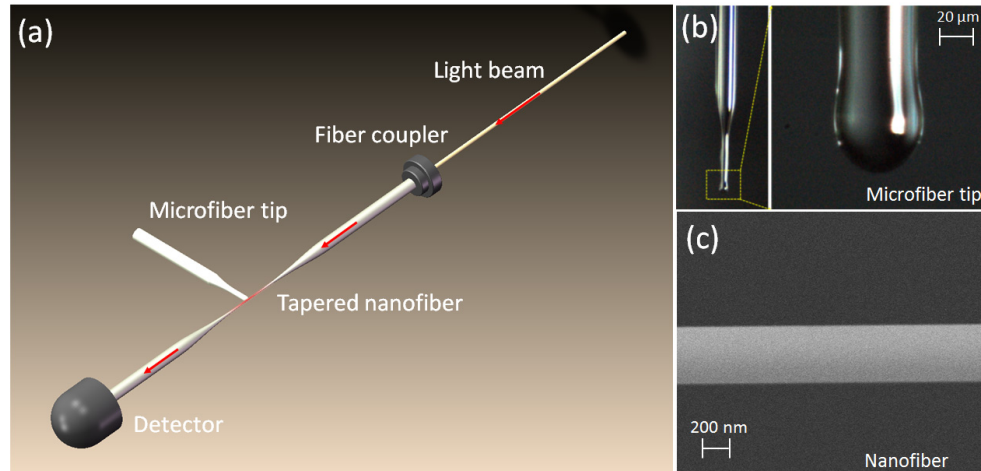


Fig. 3. (a) Schematic diagram of the experimental setup; (b) camera images of MFT; (c) typical SEM image of a nanofiber.

Figure 3(b) shows camera images of the hemispherical MFT used in our experiments, which was fabricated by a CO₂ laser with a wavelength of 10.6 μm. The CO₂ laser can melt silica optical fibers owing to the strong temperature dependence of the silica optical extinction coefficient. First, the fiber diameter was narrowed by pulling the melted optical fiber, and the narrowed fiber cut using a commercial optical fiber cleaver, resulting in a thin fiber tip with a flat endface. Next, the CO₂ laser beam was focused again and melted the flat end of the tip, and a hemispherical end formed due to the surface tension of silica. A hemispherical MFT with a diameter of 52.0 μm was utilized in the following experiments. The hemispherical MFT was positioned on a three-axis piezo stage with nanometer resolution (P-611.3 NanoCube XYZ Piezo Stage, Physik Instrumente). The length of MFT shown in Fig. 3 (b) is less than 1mm relative to where it is anchored. The setup is kept inside a two-layer glass cover to avoid the effect of air currents and dust. The MFT was moved to just touch the nanofiber with high spatial resolution. To determine the MFT-induced scattering loss, we measured the transmitted power P_1 and P_2 of the nanofiber with the MFT touching and not touching, and obtained the normalized nanofiber transmission $T = P_1 / P_2 < 1$. Owing to the much larger size of the MFT compared to the nanofiber, the method is robust against the alignment of the MFT to the nanofiber along the axis perpendicular to the nanofiber.

Experimentally, we fabricated a nanofiber with a waist diameter of approximately 670 nm, and the transmission of the nanofiber was monitored by an 852-nm laser. We moved the MFT to change the touching positions along the axis of the nanofiber and measured the normalized nanofiber transmission shown in Fig. 4(a). The theoretical curve of nanofiber transmission as a function of nanofiber diameter shown in Fig. 2(a) with a MFT diameter of 52.0 μm was used to calibrate the values of the normalized nanofiber transmission shown in Fig. 4(a), and we obtained the nanofiber diameter as a function of position along the axis of the nanofiber. We plot the nanofiber diameter versus position (black solid squares) in Fig. 4(b) and we also show the nanofiber diameter measured by SEM for comparison (red solid circles). We analyze the grey-scale SEM images digitally. In the SEM images, the gray level of nanofiber is a step which is higher than the background. We make the points with 90% of

the nanofiber's maximum gray level as the boundary of the nanofiber and get the nanofiber diameters. The gray level with 90% of the maximum is around twice of the background average noise for most cases, which is similar to the situation in [25]. The blue solid line is the theoretical curve based on the theoretical formula, $R(z) = R_0 \exp(-z/L)$, given in [26]. This formula shows the function of tapered nanofiber radius R_0 as nanofiber position z . R_0 is the original radius of the nanofiber, while L is the constant heating length. The two sets of data can be statistically compared, and both of them agree with each other and theoretical prediction. The error bars in Fig. 4(b) are derived from the standard deviation of three measurements. In the waist region, the average difference between the data measured by the two methods is 17.7 nm. The reasons for the differences can be attributed to the measurement error, imperfections of the experimental setup, and the Au coating applied before SEM measurements. The average standard deviation for the scattering-loss method is 9.8 nm (1.5% of d_{fiber}), while it is 10.2 nm for the SEM method. Imperfections of the experimental setup include the unideal hemisphere of the MFT and the power fluctuation of the laser source. The thickness of the Au coating for the SEM measurement is approximately 10 nm. There are two main reasons cause the uncertainty of 1.5%. One is the uncertainty from the power fluctuation of laser beam. We did not use an optical fiber splitter for transmission calibration in our experiment. The optical power fluctuation of the laser used in our experiment is 0.5%. Another one is the uncertainty from over-touching of the nanofiber and the MFT. If the MFT touches the nanofiber too much, the touching point becomes a short touching line, which will cause some extra scattering loss and that would increase the uncertainty. In the tapered region, the deviations between the two methods increase with increasing tapered fiber diameter. The green open circles shown in Fig. 4 (b) indicate the deviation of measured diameters by scattering-loss method and SEM method. We suspect that the reason for the deviation is the influence of high-order modes in the tapered region of the nanofiber. In obtaining our theoretical simulation results presented above, we always used the guided modes with fundamental HE_{11} modes (TE or TM modes); however, multi-modes can be guided in the tapered nanofiber with a larger diameter and interference between modes may occur in the experiments. We used the simulation results with fundamental HE_{11} modes to calibrate the tapered region, which is the reason the deviations occurred in the tapered region. Nanofibers reach single-mode region when the diameter is smaller than 621.2 nm for the wavelength 852 nm according to the single-mode condition $V = \frac{\pi D}{\lambda} \sqrt{n_{core}^2 - n_{clad}^2} < 2.405$. V is the normalized frequency and D is the nanofiber diameter. n_{core} and n_{clad} are the refractive index of the core and the cladding, respectively. The measurement results are similar to the results in [25]. In these methods, the deviations in the region with thin diameters are small, and the deviations increase in the region with thicker diameters due to the simplicity of theoretical model in which only the fundamental HE_{11} mode is considered. In our method, three repetitions give a bigger measurement uncertainty than that in [25], while [25] gives a subnanometer radial resolution by a long-time average. The measurement uncertainty of our method can be improved by increasing measurement time simply.

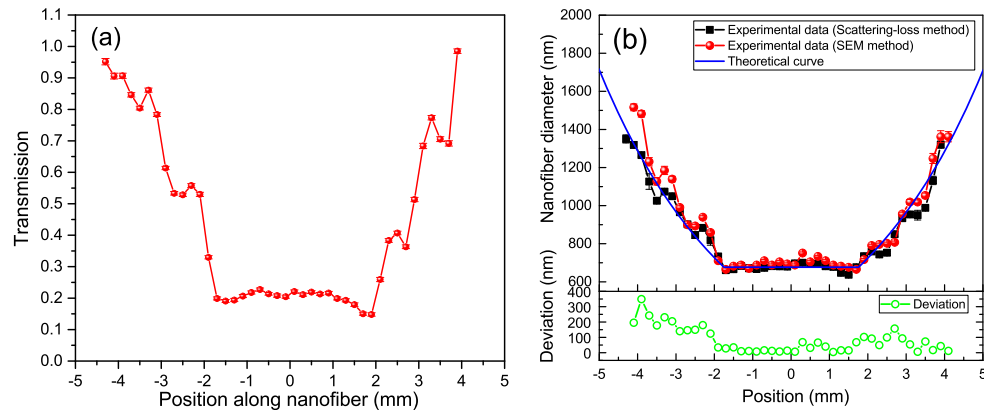


Fig. 4. (a) Measured nanofiber transmission as a function of position along axis of nanofiber. (b) Nanofiber diameter as a function of position along the axis of nanofiber measured by two methods: scattering-loss method (black solid squares) and SEM method (red solid circles). Blue solid curve is theoretical curve. The green open circles indicate the deviation of measured diameters by scattering-loss method and SEM method.

To prove the feasibility of this method, we fabricated another nanofiber sample with a waist diameter of approximately 310 nm. Figure 5(a) shows the measured values of the normalized nanofiber transmission as a function of nanofiber position with the MFT touching along the nanofiber using lasers of wavelength 852 nm (blue solid squares) and 1064 nm (red solid circles), respectively. The nanofiber is also characterized by SEM, with the results shown by orange solid circles in Fig. 5(a). We can see that the nanofiber transmission decreases with decreasing nanofiber diameter. For 852 and 1064 nm, the nanofiber transmissions both drop to their lowest values (almost zero) and increase with decreasing nanofiber diameter. We obtained experimental results that are the same as the results predicted by theoretical simulations shown in Fig. 2. For 852 nm and 1064 nm, the curves of the nanofiber transmission as a function of the nanofiber diameter shown in Fig. 5(a) are not monotonic. In Fig. 5(a), for the data around the bottom of the curve (corresponds to the minimum of the nanofiber transmission), the precision of the estimation of the fiber diameters according to the transmission is low, because the slope of the nanofiber transmission is small around the minimum. Therefore, we used another way to show the experimental data. Based on the theoretical simulation results and the experimental data, we plot the nanofiber transmission as a function of the nanofiber diameter in Fig. 5(b). The nanofiber diameter for the experimental data is from the measurement results obtained by SEM. The results are compared with the theoretical simulation. The dashed and dashed-dotted lines are the theoretical simulation results, while the blue solid squares and red solid circles are the experimental results for 852 and 1064 nm, respectively. It can be seen that the experimental data are good in agreement with theoretical simulation.

The time for measuring one sample is around one and a half hours. During the measurement the nanofiber is touched by the MFT for more than 120 times. We did not see any observable loss of the fiber during this time. The cleanliness for both of the MFT and the nanofiber have significant effect on the diameter measurements. A dust sticking at the touching point can change the nanofiber transmission totally when the MFT touches. In our experiment, we keep the setup inside a two-layer glass cover in a clean room to avoid dust. Point touching makes this method full nondestructive.

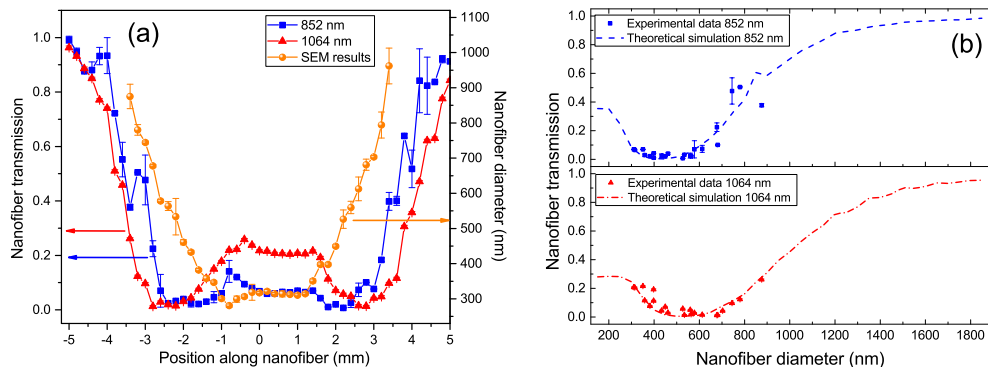


Fig. 5. (a) Normalized nanofiber transmission as function of nanofiber position with MFT touched along the nanofiber. Blue solid squares and red solid circles correspond to the data using lasers with working wavelengths of 852 and 1064 nm, respectively. Inset shows diameter profile of the sample measured by SEM (orange solid circles). (b) Nanofiber transmission as a function of nanofiber diameter measured by SEM for working wavelengths of 852 and 1064 nm.

4. Conclusions

In conclusion, we proposed and demonstrated a nondestructive, convenient, and simple method to determine nanofiber diameters based on a near-field probe and scattering-loss monitoring. In our experiment, a MFT with a hemispherical diameter of $52.0\ \mu\text{m}$ was utilized to touch the nanofibers, and induced a scattering loss of the nanofiber. The near-field-probe-induced scattering loss can be precisely calibrated by numerical simulations, and the diameter of the nanofiber can be determined by the experimental transmission data with an uncertainty of only 9.8 nm (1.5% of the measured diameter). In addition, the results obtained by our approach are in good agreement with SEM results. It is necessary to use an optical fiber splitter for normalization of the transmission and to stabilize the optical power to improve measurement uncertainties in the future. Since a MFT with a large diameter can be fabricated easily and can be measured precisely, our convenient and simple approach can be easily implemented in experiments and will boost the performance of nanofibers in their applications.

Appendix

TE and TM modes

TM mode is of the quasi-linear polarization along the x-axis of fundamental HE_{11} mode family, while TE mode is along the y-axis. We have used a commercial software (FDTD solutions, Lumerical Solutions, Inc.) to numerically simulate the nanofiber transmission with a hemispherical MFT touching and get the simulation results shown in Fig. 2 (c). From Fig. 2(c) it can be seen that polarizations of the guided mode have a very small effect on the nanofiber transmission for $d_{ip} = 52\ \mu\text{m}$. An intuitive understanding is that the size of the MFT ($52\ \mu\text{m}$) is much larger than that of the nanofiber (less than $1\ \mu\text{m}$). The guided mode is weak dependent on the polarization. The huge MFT has equivalent effect on the scattering loss whatever the polarization of the nanofiber is, so that the scattering loss is insensitive to the polarization of the light.

In order to validate the simulation results, we have experimentally measured the nanofiber transmission with the MFT touched as a function of the polarization in the nanofiber. The laser beam passes a Glan-Taylor prism and a rotary half waveplate, and we can get a laser beam with better high linear rotary polarization degree. The laser beam is collimated and coupled into an optical single mode fiber by a fiber coupler. The polarization of the light

beam in the nanofiber is controlled by the rotary half waveplate before the fiber coupler and a fiber polarization controller (FPC030, Thorlabs).

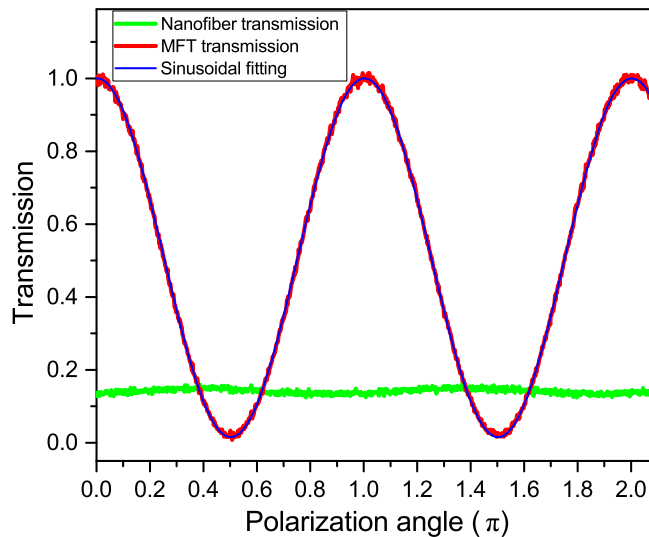


Fig. 6. Nanofiber transmission with the MFT touched as a function of the polarization before the fiber coupler. The green line is the fiber transmission. The red line is the MFT transmission from scattering photon collected by the MFT. The blue line is sinusoidal fitting.

We have plotted the nanofiber transmission as a function of the polarization before the fiber coupler in the Fig. 6. The green line is the fiber transmission. The red line is the scattered photon collected by the MFT, with the blue line is sinusoidal fitting. It is shown that the MFT transmission is strongly dependent on the polarization of the input light. We adjust the fiber polarization controller and rotate the half waveplate to change the polarization in the nanofiber. From the figure we can see that the polarization has almost no effect on the nanofiber transmission. The small fluctuation is due to the tiny difference between the TE- and TM-polarization predicted in Fig. 2 (c) or the optical power fluctuation of the laser beam.

Funding

National Key R&D Program of China (No. 2017YFA0304502); National Nature Science Foundation of China (NSFC) (11574187, 11634008); Fund for Shanxi “1331 Project” Key Subjects; Program of State Key Laboratory of Quantum Optics and Quantum Optics Devices (KF201809); Anhui Initiative in Quantum Information Technologies (AHY130000).

References

1. L. Zhang, J. Lou, and L. Tong, “Micronanofiber optical sensors,” *Photonic Sens.* **1**(1), 31–42 (2011).
2. K. P. Nayak, M. Sadgrove, R. Yalla, F. L. Kien, and K. Hakuta, “Nanofiber quantum photonics,” *J. Opt.* **20**(7), 073001 (2018).
3. G. Kurizki, P. Bertet, Y. Kubo, K. Mølmer, D. Petrosyan, P. Rabl, and J. Schmiedmayer, “Quantum technologies with hybrid systems,” *Proc. Natl. Acad. Sci. U.S.A.* **112**(13), 3866–3873 (2015).
4. L. Tong, R. R. Gattass, J. B. Ashcom, S. He, J. Lou, M. Shen, I. Maxwell, and E. Mazur, “Subwavelength-diameter silica wires for low-loss optical wave guiding,” *Nature* **426**(6968), 816–819 (2003).
5. L. Tong, F. Zi, X. Guo, and J. Lou, “Optical microfibers and nanofibers: a tutorial,” *Opt. Commun.* **285**(23), 4641–4647 (2012).
6. X. Wu and L. Tong, “Optical microfibers and nanofibers,” *Nanophotonics* **2**(5), 407–428 (2013).
7. P. Solano, J. A. Grover, J. E. Hoffman, S. Ravets, F. K. Fatemi, L. A. Orozco, and S. L. Rolston, “Optical nanofibers,” *Adv. At. Mol. Opt. Phys.* **66**, 439–505 (2017).
8. B. Gouraud, D. Maxein, A. Nicolas, O. Morin, and J. Laurat, “Demonstration of a memory for tightly guided light in an optical nanofiber,” *Phys. Rev. Lett.* **114**(18), 180503 (2015).
9. F. L. Kien, S. Dutta, D. Gupta, V. I. Balykin, and K. Hakuta, “Spontaneous emission of a cesium atom near a nanofiber Efficient coupling of light to guided modes,” *Phys. Rev. A* **72**(3), 032509 (2005).

10. R. Yalla, F. Le Kien, M. Morinaga, and K. Hakuta, "Efficient channeling of fluorescence photons from single quantum dots into guided modes of optical nanofiber," *Phys. Rev. Lett.* **109**(6), 063602 (2012).
11. K. P. Nayak, F. Le Kien, Y. Kawai, K. Hakuta, K. Nakajima, H. T. Miyazaki, and Y. Sugimoto, "Cavity formation on an optical nanofiber using focused ion beam milling technique," *Opt. Express* **19**(15), 14040–14050 (2011).
12. M. Sadgrove, R. Yalla, K. P. Nayak, and K. Hakuta, "Photonic crystal nanofiber using an external grating," *Opt. Lett.* **38**(14), 2542–2545 (2013).
13. K. P. Nayak, P. Zhang, and K. Hakuta, "Optical nanofiber-based photonic crystal cavity," *Opt. Lett.* **39**(2), 232–235 (2014).
14. V. I. Balykin, K. Hakuta, F. Le Kien, J. Q. Liang, and M. Morinaga, "Atom trapping and guiding with a subwavelength-diameter optical fiber," *Phys. Rev. A* **70**(1), 011401 (2004).
15. E. Vetsch, D. Reitz, G. Sagué, R. Schmidt, S. T. Dawkins, and A. Rauschenbeutel, "Optical interface created by laser-cooled atoms trapped in the evanescent field surrounding an optical nanofiber," *Phys. Rev. Lett.* **104**(20), 203603 (2010).
16. A. Goban, K. S. Choi, D. J. Alton, D. Ding, C. Lacroûte, M. Pototschnig, T. Thiele, N. P. Stern, and H. J. Kimble, "Demonstration of a state-insensitive, compensated nanofiber trap," *Phys. Rev. Lett.* **109**(3), 033603 (2012).
17. F. Warken and H. Giessen, "Fast profile measurement of micrometer-sized tapered fibers with better than 50-nm accuracy," *Opt. Lett.* **29**(15), 1727–1729 (2004).
18. J. Keloth, M. Sadgrove, R. Yalla, and K. Hakuta, "Diameter measurement of optical nanofibers using a composite photonic crystal cavity," *Opt. Lett.* **40**(17), 4122–4125 (2015).
19. U. Wiedemann, K. Karapetyan, C. Dan, D. Pritzkau, W. Alt, S. Irsen, and D. Meschede, "Measurement of submicrometre diameters of tapered optical fibres using harmonic generation," *Opt. Express* **18**(8), 7693–7704 (2010).
20. F. K. Fatemi, J. E. Hoffman, P. Solano, E. F. Fenton, G. Beadie, S. L. Rolston, and L. A. Orozco, "Modal interference in optical nanofibers for sub-Angstrom radius sensitivity," *Optica* **4**(1), 157–162 (2017).
21. S. Holleis, T. Hoinkes, C. Wuttke, P. Schneeweiss, and A. Rauschenbeutel, "Experimental stress-strain analysis of tapered silica optical fibers with nanofiber waist," *Appl. Phys. Lett.* **104**(16), 163109 (2014).
22. P. F. Jarschel, L. S. Magalhaes, I. Aldaya, O. Florez, and P. Dainese, "Fiber taper diameter characterization using forward Brillouin scattering," *Opt. Lett.* **43**(5), 995–998 (2018).
23. J. E. Hoffman, F. K. Fatemi, G. Beadie, S. L. Rolston, and L. A. Orozco, "Rayleigh scattering in an optical nanofiber as a probe of higher-order mode propagation," *Optica* **2**(5), 416–423 (2015).
24. M. Sumetsky, Y. Dulashko, J. M. Fini, A. Hale, and J. W. Nicholson, "Probing optical microfiber nonuniformities at nanoscale," *Opt. Lett.* **31**(16), 2393–2395 (2006).
25. L. S. Madsen, C. Baker, H. Rubinsztein-Dunlop, and W. P. Bowen, "Nondestructive profilometry of optical nanofibers," *Nano Lett.* **16**(12), 7333–7337 (2016).
26. T. A. Birks and Y. W. Li, "The shape of fiber tapers," *J. Lightwave Technol.* **10**(4), 432–438 (1992).